Computer Modeling in Engineering & Sciences

Tech Science Press

Doi:10.32604/cmes.2025.060855

ARTICLE

Mathematical Modeling of Leukemia within Stochastic Fractional Delay Differential Equations

Ali Raza[1,2,*], Feliz Minhós[2,3,*], Umar Shafique[4] and Muhammad Mohsin[5]

[1]Department of Physical Sciences, The University of Chenab, Gujrat, 50700, Pakistan
[2]Center for Research in Mathematics and Applications (CIMA), Institute for Advanced Studies and Research (IIFA), University of Évora, Rua Romão Ramalho, 59, Évora, 7000-671, Portugal
[3]Department of Mathematics, School of Science and Technology, University of Évora, Rua Romão Ramalho, 59, Évora, 7000-671, Portugal
[4]Department of Mathematics, National College of Business Administration and Economics, Lahore, 54660, Pakistan
[5]Center for Research and Development in Mathematics and Applications (CIDMA), Department of Mathematics, University of Aveiro, Aveiro, 3810-193, Portugal

*Corresponding Authors: Ali Raza. Email: ali@phs.uchenab.edu.pk or alimustasamcheema@gmail.com; Feliz Minhós. Email: fminhos@uevora.pt

Received: 11 November 2024; Accepted: 08 February 2025; Published: 30 June 2025

ABSTRACT: In 2022, Leukemia is the 13th most common diagnosis of cancer globally as per the source of the International Agency for Research on Cancer (IARC). Leukemia is still a threat and challenge for all regions because of 46.6% infection in Asia, and 22.1% and 14.7% infection rates in Europe and North America, respectively. To study the dynamics of Leukemia, the population of cells has been divided into three subpopulations of cells susceptible cells, infected cells, and immune cells. To investigate the memory effects and uncertainty in disease progression, leukemia modeling is developed using stochastic fractional delay differential equations (SFDDEs). The feasible properties of positivity, boundedness, and equilibria (i.e., Leukemia Free Equilibrium (LFE) and Leukemia Present Equilibrium (LPE)) of the model were studied rigorously. The local and global stabilities and sensitivity of the parameters around the equilibria under the assumption of reproduction numbers were investigated. To support the theoretical analysis of the model, the Grunwald Letnikov Nonstandard Finite Difference (GL-NSFD) method was used to simulate the results of each subpopulation with memory effect. Also, the positivity and boundedness of the proposed method were studied. Our results show how different methods can help control the cell population and give useful advice to decision-makers on ways to lower leukemia rates in communities.

KEYWORDS: Leukemia disease; stochastic fractional delayed model; stability analysis; Grunwald Letnikov Nonstandard Finite Difference (GL-NSFD); computational methods

1 Introduction

Leukemia is one of the very significant global public health problems that cut across all demographics. This disease results from abnormal or premature white blood cells, which grow unsymmetrical in the blood and interfere with the normal functioning of healthy cells. This therefore impairs immunity to infections and general well-being [1]. In [2], the authors analyzed new pharmacodynamic parameters associated with ibrutinib responses in chronic lymphocytic leukemia by prospective study in real-world patients. Mathematical modeling is integrated to predict treatment outcomes. In [3], the authors develop nonlinear Ordinary Differential Equation (ODE) models describing the population dynamics of leukemic cells as

functions of differences in feedback configurations and kinetic properties like self-renewal differentiation and division probabilities, proliferation, and death rates. The proposal extends to how these factors impact the course of leukemia. In [4], the authors attempted to mathematically describe the progression dynamics of chronic myeloid leukemia by providing a mathematical model of cloned hematopoiesis through nonlinear systems of differential equations. In [5], the authors integrated pharmacokinetic-pharmacodynamic (PKPD) models used to assess the clonal reduction potential of promising candidate drugs compared to high-dose cytarabine in the consolidation therapy of Acute Myeloid Leukemia (AML). Since the goal is to discover better alternatives. In [6], the authors described a simple model that describes an interface between leukemic cells and the body's autologous immune response in the chronic phase of chronic myelogenous leukemia (CML). The model attempts to capture the dynamic behavior of the growth of leukemic cells coupled with the immune system response over time. In [7], the authors studied a mathematical model describing Chimeric Antigen Receptor T (CAR-T) cells, leukemia tumors, and B cell competition. All interactions are studied in detail to understand the essence of their behavior. In [8], the authors presented and discussed an autologous tumor-immune response model for CML. The paper advances toward a mathematical modeling understanding of the dynamics of CML. In [9], the authors looked at a mathematical myeloid leukemia model, emphasizing the existence and stability of trivial and nontrivial equilibrium points. Stability analysis is given for the equilibrium states. In [10], the authors developed a mathematical model to analyze the interactions between leukemia stem cells with the bone marrow microenvironment. This model enables the simulation of some dynamics in the course of chronic myeloid leukemia progression dynamics. In [11], the authors presented a novel two-parameter discrete distribution by combining Poisson and Quasi-Shanker distributions. This new distribution offers enhanced modeling capabilities. In [12], the authors analyzed Leukemia as a blood cancer characterized by an excess number of white blood cells. If identified at any stage with accuracy, the treatment would be effective. In [13], the authors contributed to the improvement of further knowledge, and accuracies in diagnostic methods, and also play an important role in present times for the diagnosis and treatment of acute leukemia. In [14], the authors demonstrated how to infer from experimental measurements with live cell fluorescence labeling and flow cytometry on the growth regime and division strategy of leukemia cell populations an analytical model for which cell growth and division rates depend on powers of the size. In [15], the authors develop a mathematical model to describe the acute lymphoblastic leukemia (ALL) behavior, which includes the evolution of a leukemic clone during the treatment process. In [16], the authors implemented a new model, simulating the evolution of cancerous cells in patients with chronic lymphocytic leukemia receiving chemotherapy treatment, to capture the dynamics of treatment response and disease progression. In [17], the authors introduced a nonlinear leukemia dynamical system using a piecewise modified ABC fractional-order derivative. Conduct both theoretical and computational analyses of the model, specifically regarding crossover effects. In [18], the authors explored Chronic lymphocytic leukemia (CLL) protein-protein interaction networks using a new approach where both statistical thermodynamics and systems biology are brought together to identify proteins integral to the onset of the disease. In [19], the authors proposed an approach to the pattern recognition of ALL through the application of advanced computational deep learning techniques. Advanced computational deep learning, in this case, will focus on improving the outcome of leukemia diagnosis with complex algorithms aimed at detecting and classifying abnormal cell patterns. In [20], the authors discussed optimal control in a reaction-diffusion leukemia immune model that captures the interactions and dynamics between leukemia cells, normal cells, and CAR-T cells, including how to control leukemia growth, enhance CAR-T therapy efficacy, and preserve healthy cell populations. In [21], the authors provided a comprehensive introduction to the mechanistic mathematical and computational modeling of blood cell formation depicting aspects of both normal and pathological processes, involving basic principles and applications of modeling techniques concerning disorders related to hematopoiesis. Alsakaji et al. studied a stochastic tumor-immune

interaction model with external treatments and time delays, which is an optimal control problem [22]. Rihan et al. studied a fractional order delay differential model of a tumor-immune system with vaccine efficacy: stability, bifurcation, and control [23].

The stochastic fractional delayed methodology has significant scientific benefits because it combines stochastic processes, fractional calculus, and temporal delays to mimic complex systems more precisely. This approach uses fractional derivatives to capture memory effects, which is important in fields like biology and economics since it accounts for past effects on current conditions. Temporal delays are incorporated to provide a realistic depiction of the lag between cause and effect, while the stochastic component handles the inherent randomness in systems. Together, these elements enhance the models' predictive power and robustness across multiple domains, rendering them more realistic representations of real-world dynamics.

For the computational modeling of the study on leukemia, stochastic fractional delay differential equations (SFDDEs) were used and implemented in MATLAB software with fractions calculus and stochastic modules. To solve the computational challenges, adaptive step-sizing and parallel processing were added while maximizing speed but maintaining stable solutions. The model was validated by comparing it with analytical solutions for simplified cases, ensuring the results are robust and reliable.

The structure of the paper is as follows: Section 1 provides an overview and a detailed examination of leukemia-like diseases that have been reported in the literature. Section 2 examines the construction of the stochastic fractional delayed leukemia disease model, the resulting mathematical analysis, and the local and global levels of the model's equilibria, reproduction number, and stability analysis. The reproduction number sensitivity that we obtain from the Section 3 SFDDEs for the system. In Section 4, the stochastic fractional delayed model was examined using the Grunwald Letnikov Nonstandard Finite Difference (GL-NSFD) approach. In Section 5, the positivity and boundedness of the GL-NSFD were analyzed. In Section 6, the explicit focus is on numerical simulations and the results displayed. Final opinions offer a comprehensive synopsis of the work completed under Section 7.

2 Model Formulation

In this paper, we discussed a model that shows how leukemia spreads through three subgroups of cells. These groups are susceptible cells (S), infected cells (I), and immune cells (W). The susceptible group (S) includes cells that can get leukemia but don't have it yet. The infected group (I) has cells that have leukemia and can spread it. The immune group (W) includes cells that have recovered from leukemia and are now immune, meaning they can't get it again. Further, let Λ be the rate at which the susceptible blood cells enter the circulatory blood from compartments like bone marrow, lymph nodes, and thymus. Parameters μ, γ, and b are the natural mortality rates of susceptible blood cells, infected cells, and immune cells, respectively. The parameter β is the infection rate of susceptible blood cells. The rate at which the infected cells are recovered due to encounters with immune cells is denoted by ε.

A flow diagram of the model has been provided in Fig. 1. The basic structure for the investigations is the deterministic model introduced in [1], whereby the first-order temporal derivatives are substituted by fractional Caputo derivatives of order α. We believe that such an adjustment provides a more appropriate picture of the diffusion of leukemia disease. In the model analysis, Caputo fractional derivatives are employed to include memory on the fact that the system depends on previous user behavior, and it seems to store this information in long-term memory about other cases of leukemia. From this modification, one can see that the model is well suited to representing the processes of leukemia disease, especially over some time due to the non-linearity. The random or stochastic disturbances are incorporated to provide for the random nature and variation that is present in the systems under study. These stochastic components can facilitate and consider the complex spread of disease, as well as the unpredictable dynamics visible in the actual utilization of leukemia disease.

$$ {}_0^c D_t^\alpha [S] = \Lambda^\alpha - \beta^\alpha S(t-\tau) I(t-\tau) e^{-(\mu^\alpha+\gamma^\alpha)\tau} - \mu^\alpha S + \sigma_1^\alpha S dB(t), \tag{1} $$

$$ {}_0^c D_t^\alpha [I] = \beta^\alpha S(t-\tau) I(t-\tau) e^{-(\mu^\alpha+\gamma^\alpha)\tau} - (\gamma^\alpha + \varepsilon^\alpha) I + \sigma_2^\alpha I dB(t), \tag{2} $$

$$ {}_0^c D_t^\alpha [W] = \varepsilon^\alpha I - b^\alpha W + \sigma_3^\alpha W dB(t). \tag{3} $$

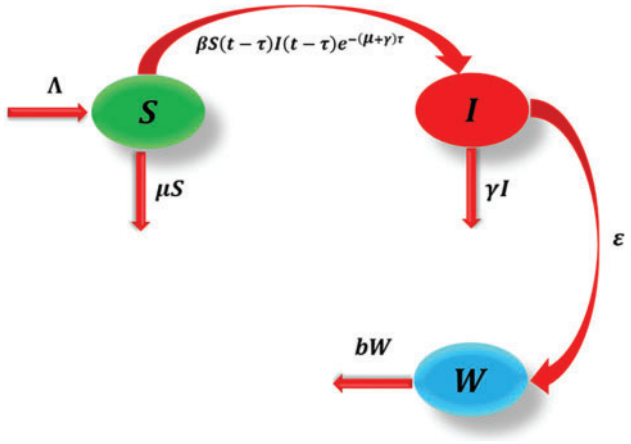

Figure 1: Flow diagram of leukemia disease

The nonnegative (initial) conditions for the system (1)–(3) are

$$ S(0) \geq 0, I(0) \geq 0, W(0) \geq 0, t \geq 0, \tau < t, $$

and

$$ N = S + I + W. $$

This strategy indicates how the random disturbances in the system can be represented by the stochastic fluctuations σ_i^α; $i = 1, 2, 3$. Let $B(t)$ be Brownian motion, a continuous stochastic process for time $t \geq 0$. The parameter τ acts as a time delay to the system provided that $\tau < t$ also so that the effect of the delayed feedback is visible only after a time interval.

Preliminaries: In the conceptualization of Caputo, the following foundational preliminary definitions are crucial for a deep and thorough understanding of the fractional derivative concept:

Definition 1: *For a function $q \in C_n$, the Caputo fractional derivative of order $\alpha \in (m-1, m)$, $m \in N$ is*

$$ {}_0^c D_t^\alpha q(t) = \frac{1}{\Gamma(m-\alpha)} \int_0^t \frac{q^m(\mathfrak{T})\, d\mathfrak{T}}{(t-\mathfrak{T})^{\alpha+1-m}}. $$

Definition 2: *For thefunction $q(t)$, the expression describes the equivalent fractional integral with order $\alpha > 0$.*

$$ I_t^\alpha q(t) = \frac{1}{\Gamma(\alpha)} \int_0^t (t-\mathfrak{T})^{\alpha-1} q(\mathfrak{T})\, d\mathfrak{T}. $$

where "Γ" is the gamma function displayed.

2.1 Existence and Uniqueness of the Stochastic Fractional Delayed Model

This section of the paper establishes the stochastic fractional delayed model's existence and uniqueness. Apply the fractional integral in this case, assuming $\sigma_i^{\alpha} = 0; i = 1, 2, 3$, under the system (1)–(3) starting condition.

$$S(t) = S_0 + \frac{1}{\Gamma(\alpha)} \int_0^t (t-s)^{\alpha-1} \hbar_1(s, S)\, dS, \tag{4}$$

$$I(t) = I_0 + \frac{1}{\Gamma(\alpha)} \int_0^t (t-s)^{\alpha-1} \hbar_2(s, I)\, ds, \tag{5}$$

$$W(t) = W_0 + \frac{1}{\Gamma(\alpha)} \int_0^t (t-s)^{\alpha-1} \hbar_3(s, W)\, ds. \tag{6}$$

The functions defined under the integral in system (4)–(6) are

$$\hbar_1(t, F) = \Lambda^{\alpha} - \beta^{\alpha} SIe^{-(\mu^{\alpha}+\gamma^{\alpha})\tau} - \mu^{\alpha} S, \tag{7}$$

$$\hbar_2(t, I) = \beta^{\alpha} SIe^{-(\mu^{\alpha}+\gamma^{\alpha})\tau} - (\gamma^{\alpha} + \varepsilon^{\alpha}) I, \tag{8}$$

$$\hbar_3(t, P) = \varepsilon^{\alpha} I - b^{\alpha} W. \tag{9}$$

Furthermore, it is assumed that $\mathcal{E}_1, \mathcal{E}_2$, and $\mathcal{E}_3$ exist as positive constants and that $S(t), I(t)$, and $W(t)$ are non-negative limiting functions, such that

$$\|S(t)\| \le \mathcal{E}_1, \|I(t)\| \le \mathcal{E}_2, \|W(t)\| \le \mathcal{E}_3.$$

Theorem 1: *The function $\hbar_i$ for $i = 1, 2, 3$ fulfills the Lipshitz requirement and are contraction mappings by assuming $\sigma_i^{\alpha} = 0; i = 1, 2, 3$, if the condition $0 \le \mathcal{W} = max\{1, 2, 3\} < 1$ is true.*

Proof: First, we consider the function $\hbar_1$. Examine the subsequent S and S_1:

$$\|\hbar_1(t, S) - \hbar_2(t, S_1)\| = \left\|\beta^{\alpha}(S - S_1) Ie^{-(\mu^{\alpha}+\gamma^{\alpha})\tau} + \mu^{\alpha}(S - S_1)\right\|,$$

$$\|\hbar_1(t, S) - \hbar_2(t, S_1)\| \le \left\|\beta^{\alpha}(S - S_1) Ie^{-(\mu^{\alpha}+\gamma^{\alpha})\tau}\right\| + \|\mu^{\alpha}(S - S_1)\|,$$

$$\|\hbar_1(t, S) - \hbar_2(t, S_1)\| \le \left(\beta^{\alpha}(S - S_1) e^{-(\mu^{\alpha}+\gamma^{\alpha})\tau} \|I\| + \mu^{\alpha}\right) \|S - S_1\|,$$

$$\|\hbar_1(t, S) - \hbar_2(t, S_1)\| \le \left(\beta^{\alpha} e^{-(\mu^{\alpha}+\gamma^{\alpha})\tau} \mathcal{E}_2 + \mu^{\alpha}\right) \|S - S_1\|,$$

$$\|\hbar_1(t, S) - \hbar_2(t, S_1)\| \le \xi_1 \|S - S_1\|. \tag{10}$$

In this instance, $\xi_1 = \left(\beta^{\alpha} e^{-(\mu^{\alpha}+\gamma^{\alpha})\tau} \mathcal{E}_2 + \mu^{\alpha}\right)$. Lipshitz's condition is satisfied. This method may also be used to meet the Lipschitz criteria for $\hbar_i$, $i = 2, 3$. Additionally, if $0 \le \mathcal{W} = max\{1, 2, 3\} < 1$, then the functions are contractions. Furthermore, there is constant writing in the system (7)–(9).

$$S_n(t) = \frac{1}{\Gamma(\alpha)} \int_0^t (t-s)^{\alpha-1} \hbar_1(s, S_{n-1})\, ds, \tag{11}$$

$$I_n(t) = \frac{1}{\Gamma(\alpha)} \int_0^t (t-s)^{\alpha-1} \hbar_2(s, I_{n-1})\, ds, \tag{12}$$

$$W_n(t) = \frac{1}{\Gamma(\alpha)} \int_0^t (t-s)^{\alpha-1} \hbar_3(s, W_{n-1})\, ds. \tag{13}$$

The two terms' variation is represented by the following in (11)–(13):

$$\psi_{n-1}(t) = (S_n(t) - S_{n-1}(t)) = \frac{1}{\Gamma(\alpha)} \int_0^t (\hbar_1(s, S_{n-1}) - \hbar_1(s, S_{n-2}))\, ds, \tag{14}$$

$$\varphi_{n-1}(t) = (I_n(t) - I_{n-1}(t)) = \frac{1}{\Gamma(\alpha)} \int_0^t (\hbar_2(s, I_{n-1}) - \hbar_2(s, I_{n-2}))\, ds, \tag{15}$$

$$\vartheta_{n-1}(t) = (W_n(t) - W_{n-1}(t)) = \frac{1}{\Gamma(\alpha)} \int_0^t (\hbar_3(s, W_{n-1}) - \hbar_3(s, W_{n-2}))\, ds. \tag{16}$$

Therefore, we have

$$S_n(t) = \sum_{i=0}^{n} \psi_i(t), \tag{17}$$

$$I_n(t) = \sum_{i=0}^{n} \varphi_i(t), \tag{18}$$

$$W_n(t) = \sum_{i=0}^{n} \vartheta_i(t). \tag{19}$$

Let,

$$\begin{aligned}
\|\psi_n(t)\| &= \|S_n(t) - S_{n-1}(t)\|, \\
\|\psi_n(t)\| &= \frac{1}{\Gamma(\alpha)} \int_0^t (\hbar_1(s, S_{n-1}) - \hbar_1(s, S_{n-2}))\, ds, \\
\|\psi_n(t)\| &= \frac{\xi_1}{\Gamma(\alpha)} \int_0^t \|S_n(t) - S_{n-1}(t)\|\, ds, \\
\|\psi_n(t)\| &= \frac{\xi_1}{\Gamma(\alpha)} \int_0^t \psi_{n-1}(t)\, ds.
\end{aligned} \tag{20}$$

The remaining equations in the system (15) and (16) might be solved using the same method to get

$$\|\varphi_n(t)\| = \frac{\xi_2}{\Gamma(\alpha)} \int_0^t \varphi_{n-1}(t)\, ds, \tag{21}$$

$$\|\vartheta_n(t)\| = \frac{\xi_3}{\Gamma(\alpha)} \int_0^t \vartheta_{n-1}(t)\, ds. \tag{22}$$

As required. □

Theorem 2: *Show that* (i) *The system (14)–(16) has a specified uniform function.* (ii) *If there is a* $t_* > 1$ *such that* $\frac{\xi_1}{\Gamma(\alpha)} < 1$. *Assuming* $\sigma_i^{\alpha} = 0; i = 1, 2, 3$, *the model system has at least one solution if* $\frac{\xi_1}{\Gamma(\alpha)} < 1$ *for* $i = 1, 2, 3$.

Proof: Since each kernel $\hbar_1$ for $i = 1, 2, 3$, satisfies the Lipschitz condition and the functions $S(t), I(t),$ and $W(t)$ are bounded, the following relations may be determined.

$$\|\psi_n(t)\| \le \|S(0)\| \left\| \frac{\xi_1}{\Gamma(\alpha)}(t) \right\|^n, \tag{23}$$

$$\|\vartheta_n(t)\| \le \|I(0)\| \left\| \frac{\xi_2}{\Gamma(\alpha)}(t) \right\|^n, \tag{24}$$

$$\|\psi_n(t)\| \le \|W(0)\| \left\| \frac{\xi_3}{\Gamma(\alpha)}(t) \right\|^n. \tag{25}$$

In the system (23)–(25) figure, it is demonstrated that the function given in (17)–(19) exists and is consistent. It is necessary to show that $S(t), I(t),$ and $W(t)$ converge to the system of solutions of (1)–(3) to prove (ii). To do this, we define the remaining terms after n changes as $A_n(t), B_n(t),$ and $C_n(t)$. Thus,

$$S(t) - S(0) = S_n(t) - A_n(t), \tag{26}$$

$$I(t) - I(0) = I_n(t) - B_n(t), \tag{27}$$

$$W(t) - W(0) = W_n(t) - C_n(t). \tag{28}$$

By using the ξ_1 Lipschitz condition and the triangle inequality, we obtain to determine that

$$\|A_n(t)\| = \frac{1}{\Gamma(\alpha)} \int_0^t (\hbar_1(s, S_{n-1}) - \hbar_1(s, S_{n-2}))\, ds,$$

$$\|A_n(t)\| \leq \frac{\xi_1}{\Gamma(\alpha)} \|S_n(t) - S_{n-1}(t)\|. \tag{29}$$

When the process in (29) is repeated, we obtain

$$\|A_n(t)\| \leq \left\| \frac{\xi_1}{\Gamma(\alpha)}(t) \right\|^{n+1} \mathcal{E}_1. \tag{30}$$

Next, at t_*, one acquires

$$\|A_n(t)\| \leq \left\| \frac{\xi_1}{\Gamma(\alpha)}(t_*) \right\|^{n+1} \mathcal{E}_1. \tag{31}$$

Assuming $n \to \infty$ as the limit,

$$\lim_{n\to\infty} \|A_n(t)\| \leq \lim_{n\to\infty} \left\| \frac{\xi_1}{\Gamma(\alpha)}(t_*) \right\|^{n+1} \mathcal{E}_1. \tag{32}$$

By applying the hypothesis $\frac{\xi_1}{\Gamma(\alpha)}(t_*) < 1$, we have from (32) yield.

$$\lim_{n\to\infty} \|A_n(t)\| = 0. \tag{33}$$

By using the same process as for $n \to \infty$, we get

$$\|B_n(t)\| \to 0, \tag{34}$$

$$\|C_n(t)\| \to 0. \tag{35}$$

As a result, there must be only one solution.

As desired. □

Theorem 3: *If* $\left(1 - \frac{\xi_1}{\Gamma(\alpha)}(t)\right) > 0$ *for the assumption* $\sigma_i^\alpha = 0; i = 1, 2, 3,$ *then the system (1)–(3) has a unique solution.*

Proof: Consider that another collection of solutions to (1)–(3) is represented by the sets $S_1, I_1,$ and W_1.

$$\|S(t) - S_1(t)\| = \frac{1}{\Gamma(\alpha)} \int_0^t (\hbar_1(s, S_{n-1}) - \hbar_1(s, S_{n-2}))\, ds,$$

$$\|S(t) - S_1(t)\| \leq \frac{\xi_1}{\Gamma(\alpha)} \|S(t) - S_1(t)\|. \tag{36}$$

If the terms in (36), are rearranged, one gets

$$\left(1 - \frac{\xi_1}{\Gamma(\alpha)}(t)\right) \|S(t) - S_1(t)\| \leq 0, \tag{37}$$

By applying the hypothesis $\left(1 - \frac{\xi_1}{\Gamma(\alpha)}(t)\right) > 0$, we have from (37) yield.

$$\|S(t) - S_1(t)\| = 0. \tag{38}$$

It follows from this because $S(t) = S_1(t)$. Applying the identical process to every solution for $i = 2, 3$, we arrive at

$$I(t) = I_1(t), \tag{39}$$
$$W(t) = W_1(t). \tag{40}$$

Hence proved. □

Theorem 4: *For the initial conditions with assumption* $\sigma_i^\alpha = 0; i = 1, 2, 3$, *prove that the stochastic fractional delayed model (1)–(3) has a positive solution in* $\mathbb{R}^{+3}$.

Proof: The feasible situation must be non-negative across the system to be considered under the initial condition. We obtain

${}_0^c D_t^\alpha [S(t)]|_{S=0} = \Lambda^\alpha > 0$, ${}_0^c D_t^\alpha [I(t)]|_{I=0} = \beta^\alpha S I e^{-(\mu^\alpha + \gamma^\alpha)\tau} > 0$, ${}_0^c D_t^\alpha [W(t)]|_{W=0} = \varepsilon^\alpha I > 0$,

hence, the stochastic fractional delayed model (1)–(3) has a positive solution, when the initial condition falls inside the feasible region. □

Theorem 5: *The system (1)–(4) in the feasible region* $\mathcal{G} = \left\{ (S(t), I(t), W(t)) \in \mathbb{R}^{+3}; 0 < N \leq \frac{\Lambda^\alpha}{\mu^\alpha}, \forall t \geq 0, \tau < t \right\}$; *(where* $N(t) = S(t) + I(t) + W(t)$*) at any given time* t. *The initial condition is bounded with the assumption that* $\sigma_i^\alpha = 0; i = 1, 2, 3$.

Proof: The total sum of plant population can be written as

$${}_0^c D_t^\alpha N(t) \leq \Lambda^\alpha - \mu^\alpha N(t).$$

After resolving the inequality above, we obtain

$$N(t) \leq \frac{\Lambda^\alpha}{\mu^\alpha} + \left(N(0) - \frac{\Lambda^\alpha}{\mu^\alpha}\right) e^{-\mu^\alpha t}.$$

Using Grown's inequality

$$\lim_{t \to \infty} Sup N(t) \leq \frac{\Lambda^\alpha}{\mu^\alpha}. \tag{41}$$

Therefore, the epidemiologically feasible region for the propagation of cassava mosaic disease is provided by (41).

$$\mathcal{G} = \left\{ (S(t), I(t), W(t)) \in \mathbb{R}^{+3}; 0 < N \leq \frac{\Lambda^{\alpha}}{\mu^{\alpha}}, \forall t \geq 0, \tau < t \right\}. \tag{42}$$

The stochastic fractional delayed model (1)–(3) is both positively invariant and realistic from an epidemiological point of view concerning the transmission of leukemia disease (42). Hence, the system (1)–(3) is bounded under the initial conditions. □

2.2 Model Equilibria and Reproduction Number

In this part, we examine the different states of the stochastic fractional delayed model (1)–(3) with the propagation of leukemia disease dynamics. It allows the analysis of the system behavior and how the system behaves at the free and present state of the leukemia equilibrium. It also provided information on how the fractional order, delays, and stochastic parameters behave and control the transmission of leukemia disease using different numerical techniques. Therefore,

$$\text{Leukemia Free Equilibrium} = LFE = \mathcal{C}^0 = (S_0, I_0, W_0) = \left(\frac{\Lambda^{\alpha}}{\mu^{\alpha}}, 0, 0 \right), \tag{43}$$

$$\text{Leukemia Present Equilibrium} = LPE = \mathcal{C}^* = (S^*, I^*, W^*), \tag{44}$$

$$S^* = \frac{(\gamma^{\alpha} + \varepsilon^{\alpha})}{\beta^{\alpha} e^{-(\mu^{\alpha}+\gamma^{\alpha})\tau}}, I^* = \frac{\Lambda^{\alpha}\beta^{\alpha} e^{-(\mu^{\alpha}+\gamma^{\alpha})\tau} - \mu^{\alpha}(\gamma^{\alpha} + \varepsilon^{\alpha})}{\beta^{\alpha} e^{-(\mu^{\alpha}+\gamma^{\alpha})\tau}(\gamma^{\alpha} + \varepsilon^{\alpha})}, W^* = \frac{\varepsilon^{\alpha}}{b^{\alpha}} I^*$$

In epidemiology, the basic reproduction number is an important parameter. This suggests whether or not the disease is prevalent in the general population. If the value of it is less, then the disease is not spreading in the population, otherwise, the disease is present in the population. For the evaluation of the reproduction number using the Next-generation method. The largest eigenvalue or spectral radius of, at leukemia-free equilibrium (43) called reproduction number as follows:

$$R_0 = \frac{\Lambda^{\alpha}\beta^{\alpha} e^{-(\mu^{\alpha}+\gamma^{\alpha})\tau}}{\mu^{\alpha}(\gamma^{\alpha} + \varepsilon^{\alpha})}. \tag{45}$$

Theorem 6: *Assuming* $\sigma_i^{\alpha} = 0; i = 1, 2, 3$, *the leukemia-free equilibrium (43) is locally asymptotically stable for* $\alpha \in (0, 1)$ *if* $R_0 < 1$.

Proof: By linearizing the stochastic fractional delayed model (1)–(3) about (43) a 3 × 3 dimensional Jacobian matrix with negative real components and eigenvalues is obtained.

$\lambda_1 = -\mu^{\alpha}, \lambda_2 = -b^{\alpha}, \lambda_3 = -(\gamma^{\alpha} + \varepsilon^{\alpha})(1 - R_0)$.

As a result, the leukemia-free equilibrium of the provided stochastic fractional delayed model (1)–(3) is locally stable if $R_0 < 1$. If $R_0 > 1$, then (43) is unstable in the local sense. □

Theorem 7: *Assuming* $\sigma_i^{\alpha} = 0; i = 1, 2, 3$, *the stochastic fractional delayed model (1)–(3) is globally asymptotically stable (GAS) at leukemia-free equilibrium,* $\mathcal{C}^0$ *if* $R_0 < 1$.

Proof: Define the Lyapunov function $\mathcal{L}: \mathcal{G} \to \mathbb{R}$ defined as

$$\mathcal{L}(t) = \left[S - S_0 - S_0 log \frac{S}{S_0} \right] + I + W,$$

$$
\begin{aligned}
&{}_0^cD_t^\alpha \mathcal{L}(t) = \left[\frac{S-S_0}{S}\right] D_t^\alpha S + D_t^\alpha I + D_t^\alpha W,\\
&{}_0^cD_t^\alpha \mathcal{L}(t) = \left[\frac{S-S_0}{S}\right]\left(\Lambda^\alpha - \beta^\alpha SIe^{-(\mu^\alpha+\gamma^\alpha)\tau} - \mu^\alpha S\right) + \left(\beta^\alpha SIe^{-(\mu^\alpha+\gamma^\alpha)\tau} - (\gamma^\alpha+\varepsilon^\alpha) I\right) + (\varepsilon^\alpha I - b^\alpha W),\\
&{}_0^cD_t^\alpha \mathcal{L}(t) \le -\Lambda^\alpha \frac{(S-S_0)^2}{SS_0} - \gamma^\alpha I\left(1 - \frac{\beta^\alpha Se^{-(\mu^\alpha+\gamma^\alpha)\tau}}{\gamma^\alpha}\right) - b^\alpha W.
\end{aligned}
$$

This implies that ${}_0^cD_t^\alpha \mathcal{L} \le 0$ if $R_0 < 1$ and ${}_0^cD_t^\alpha \mathcal{L} = 0$ if $S(t) = S_0, I(t) = W(t) = 0$. Therefore, $\mathcal{C}^0$ is globally asymptotically stable. □

Theorem 8: *Assuming* $\sigma_i^\alpha = 0; i = 1,2,3$, *the leukemia-present equilibrium (44) is locally asymptotically stable for* $\alpha \in (0,1)$ *if* $R_0 > 1$.

Proof: By linearizing the stochastic fractional delayed model (1)–(3) about (44) a 3 × 3 dimensional Jacobian matrix with negative real components and eigenvalues is obtained.

$$
\begin{aligned}
&\lambda_1 = -b^\alpha,\\
&\lambda^2 + a_1\lambda + a_0 = 0,\\
&a_1 = \mu^\alpha + \beta^\alpha S^* e^{-(\mu^\alpha+\gamma^\alpha)\tau}, a_0 = \mu^\alpha(\gamma^\alpha+\varepsilon^\alpha)(R_0-1) + (\gamma^\alpha+\varepsilon^\alpha)\left(2\mu^\alpha + \beta^\alpha I^* e^{-(\mu^\alpha+\gamma^\alpha)\tau}\right).
\end{aligned}
$$

As a result, the leukemia-present equilibrium of the provided stochastic fractional delayed model (1)–(3) is locally stable if $R_0 > 1$. If $R_0 < 1$, then (1)–(3) is unstable in the local sense. □

Theorem 9: *Assuming* $\sigma_i^\alpha = 0; i = 1,2,3,4$, *the stochastic fractional delayed model (1)–(4) is globally asymptotically stable (GAS) at leukemia present equilibrium,* $\mathcal{C}^*$ *if* $R_0 > 1$.

Proof: Define the Lyapunov function $Z: \mathcal{G} \to \mathbb{R}$ defined as

$$
Z = k_1\left(S - S^* - S^*\ln\left(\frac{S}{S^*}\right)\right) + k_2\left(I - I^* - I^*\ln\left(\frac{I}{I^*}\right)\right) + k_3\left(W - W^* - W^*\ln\left(\frac{W}{W^*}\right)\right).
$$

Given positive constants $k_i (i = 1,2,3)$, we can express the following equation:

$$
\begin{aligned}
&{}_0^cD_t^\alpha Z = k_1\left[\frac{S-S^*}{S}\right] D_t^\alpha S + k_2\left[\frac{I-I^*}{I}\right] D_t^\alpha I + k_3\left[\frac{W-W^*}{W}\right] D_t^\alpha W,\\
&{}_0^cD_t^\alpha Z = -k_1\Lambda^\alpha \frac{(S-S^*)^2}{SS^*} - k_2\beta^\alpha SIe^{-(\mu^\alpha+\gamma^\alpha)\tau}\frac{(I-I^*)^2}{II^*} - k_3\varepsilon^\alpha I\frac{(W-W^*)^2}{WW^*}.
\end{aligned}
$$

If we choose k_i where $(i = 1,2,3)$

$$
{}_0^cD_t^\alpha Z = -\Lambda^\alpha \frac{(F-F^*)^2}{FF^*} - \beta^\alpha SIe^{-(\mu^\alpha+\gamma^\alpha)\tau}\frac{(I-I^*)^2}{II^*} - \varepsilon^\alpha I\frac{(W-W^*)^2}{WW^*}.
$$

${}_0^cD_t^\alpha Z \le 0$, for $R_0 > 1$ and ${}_0^cD_t^\alpha Z = 0$ if and only if $S = S^*, I = I^*, W = W^*$. Hence by Lasalle's invariance principle (44) is globally asymptotical stable. □

3 Sensitivity Analysis

In this section, we examine the behavior of model parameters concerning reproduction number R_0. Examine the transmission and spread of disease with the sensitive analysis of the model. Preliminary: The formalized sensitivity index of a variable Θ, that depends differentiable on a parameter ϱ:

$$\mathcal{E}_{\varrho}^{\mathrm{e}} = \frac{\varrho}{\mathrm{e}} \times \frac{\partial \mathrm{e}}{\partial\, \varrho}.$$

In spatial terms, determine the sensitive indices of parameters concerning the reproduction number R_0.

$$\mathbb{V}_{\Lambda^\alpha} = \frac{\Lambda^\alpha}{R_0} \times \frac{\partial R_0}{\partial \Lambda^\alpha} = 1 > 0, \mathbb{V}_{\beta^\alpha} = \frac{\beta^\alpha}{R_0} \times \frac{\partial R_0}{\partial \beta^\alpha} = 1 >, \mathbb{V}_{\mu^\alpha} = \frac{\mu^\alpha}{R_0} \times \frac{\partial R_0}{\partial \mu^\alpha} = -\frac{1}{\mu^\alpha} < 0,$$

$$\mathbb{V}_{\gamma^\alpha} = \frac{\gamma^\alpha}{R_0} \times \frac{\partial R_0}{\partial \gamma^\alpha} = -\frac{1}{(\gamma^\alpha + \varepsilon^\alpha)} < 0, \mathbb{V}_{\varepsilon^\alpha} = \frac{\varepsilon^\alpha}{R_0} \times \frac{\partial R_0}{\partial \varepsilon^\alpha} = -\frac{1}{(\gamma^\alpha + \varepsilon^\alpha)} < 0.$$

Tables 1 and 2 provide the values of the sensitivity indicators together with the uncertainty indicators. All the parameters $(\Lambda^\alpha, \beta^\alpha)$ have positive sensitivity values. This means that the parameters have raised the value of R_0 it becomes possible to make it high, hence making the system out of control. These parameters could represent transmission rates or factors that enhance the spread of the condition. The parameters $(\mu^\alpha, \gamma^\alpha, \varepsilon^\alpha)$ associated with negative sensitivity values suggest that a higher value of these parameters results in a lower R_0. These parameters probably measure natural mortality rates of susceptible blood cells, infected cells, and infected cells recovered due to encounters with immune cells which decrease the persistence or spread of the condition. For instance, if $\mu^\alpha = -2, \gamma^\alpha = -1.996, \varepsilon^\alpha = -1.9996$, the model also illustrates that such parameters' increase would imply a remarkably reduced reproduction number, which underlines the importance of recovery or intervention mechanisms. Fig. 2 shows how different parameters affect R_0. When increased, the parameters with negative sensitivity like $(\mu^\alpha, \gamma^\alpha, \varepsilon^\alpha)$ decrease R_0, and therefore the spread of the disease can be minimized if either recovery improves, or transmission is less. Conversely, those factors that lead to higher values of sensitivity parameters $(\Lambda^\alpha, and \beta^\alpha)$ are indicative of factors that raise the value of R_0.

Table 1: Parameters sensitivity signs

Parameters	Signs
$\boldsymbol{\Lambda^\alpha}$	Positive
$\boldsymbol{\beta^\alpha}$	Positive
$\boldsymbol{\mu^\alpha}$	Negative
$\boldsymbol{\gamma^\alpha}$	Negative
$\boldsymbol{\varepsilon^\alpha}$	Negative

Table 2: Parameters sensitivity values

Parameters	Values
$\boldsymbol{\Lambda^\alpha}$	1
$\boldsymbol{\beta^\alpha}$	1
$\boldsymbol{\mu^\alpha}$	−2
$\boldsymbol{\gamma^\alpha}$	−1.996
$\boldsymbol{\varepsilon^\alpha}$	−1.996

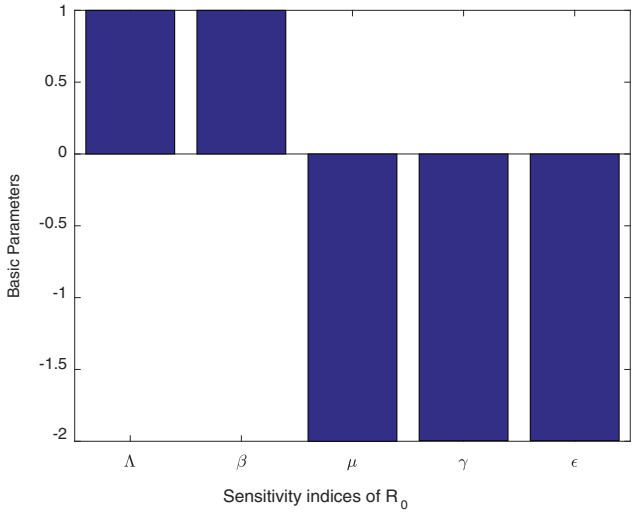

Figure 2: Sensitivity indices of reproduction number (R_0)

4 Stochastic Fractional Delayed GL-NSFD Method

This section presents a numerical method for the stochastic fractional delayed model (1)–(3) that underlies it. Another instance of the stochastic fractional delayed system is provided.

$$ {}_0^c D_t^\alpha [S]|_{t=t_n} = \Lambda^\alpha - \beta^\alpha S_{n+1} I_n e^{-(\mu^\alpha+\gamma^\alpha)\tau} - \mu^\alpha S_{n+1} + \sigma_1^\alpha S_n dB(t), \tag{46} $$

$$ {}_0^c D_t^\alpha [I]|_{t=t_n} = \beta^\alpha S_{n+1} I_n e^{-(\mu^\alpha+\gamma^\alpha)\tau} - (\gamma^\alpha + \varepsilon^\alpha) I_{n+1} + \sigma_2^\alpha I_n dB(t), \tag{47} $$

$$ {}_0^c D_t^\alpha [W]|_{t=t_n} = \varepsilon^\alpha I_{n+1} - b^\alpha W_{n+1} + \sigma_3^\alpha W_n dB(t). \tag{48} $$

First, the Grunwald-Letnikove approach, or GL is explained:

$$ {}_0^c D_t^\alpha \upsilon(t)|_{t=t_n} = \frac{1}{(\mathcal{K}(\Delta t))^\alpha} \left(\mathcal{K}_{n+1} - \sum_{i=1}^{n+1} \nu_i \mathcal{K}_{n+1-i} - \rho_{n+1} \mathcal{K}_0 \right), \tag{49} $$

here,

$$ \nu_i = (-1)^{i-1} \begin{pmatrix} \alpha \\ i \end{pmatrix} \nu_1 = \alpha, $$

$$ \rho_i = \frac{i^{-\alpha}}{\Gamma(1-\alpha)}; i = 1, 2, 3, \ldots, n+1. $$

Now, the outcome that follows helps verify some other hypotheses.

NSFD rules are added to the GL approach, making the discrete model for susceptible cells as

$$ \frac{1}{(\mathcal{K}(h))^\alpha} \left(S_{n+1} - \sum_{i=1}^{n+1} \nu_i S_{n+1-i} - \rho_{n+1} S_0 \right) = \Lambda^\alpha - \beta^\alpha S_{n+1} I_n e^{-(\mu^\alpha+\gamma^\alpha)\tau} - \mu^\alpha S_{n+1} + \sigma_1^\alpha S_n \Delta B n, \tag{50} $$

$$ S_{n+1} = \frac{\sum_{i=1}^{n+1} \nu_i S_{n+1-i} - \rho_{n+1} S_0 + (\mathcal{K}(h))^\alpha (\Lambda^\alpha + \sigma_1^\alpha S_n \Delta B n)}{1 + (\mathcal{K}(h))^\alpha (\beta^\alpha I_n e^{-(\mu^\alpha+\gamma^\alpha)\tau} + \mu^\alpha)}. \tag{51} $$

Additionally, the latent and breaking out susceptible GL-NSFD scheme as

$$I_{n+1} = \frac{\sum_{i=1}^{n+1} \nu_i I_{n+1-i} + \rho_{n+1} I_0 + (\mathcal{K}(h))^{\alpha} \left(\beta^{\alpha} S_{n+1} I_n e^{-(\mu^{\alpha}+\gamma^{\alpha})\tau} + \sigma_2^{\alpha} I_n \Delta Bn\right)}{1 + (\mathcal{K}(h))^{\alpha} (\gamma^{\alpha} + \varepsilon^{\alpha})}, \tag{52}$$

$$W_{n+1} = \frac{\sum_{i=1}^{n+1} \nu_i W_{n+1-i} + \rho_{n+1} W_0 + (\mathcal{K}(h))^{\alpha} (\varepsilon^{\alpha} I_{n+1} + \sigma_3^{\alpha} W_n \Delta Bn)}{1 + (\mathcal{K}(h))^{\alpha} (b^{\alpha})}. \tag{53}$$

5 Positivity and Boundedness of Stochastic Fractional Delayed GL-NSFD

The positivity and boundedness of the solution for the systems (1)–(3) are confirmed by the following theorem.

Theorem 10: *Suppose that* $S_0 \geq 0, I_0 \geq 0, W_0 \geq 0, \Lambda^{\alpha} \geq 0, \beta^{\alpha} \geq 0, \mu^{\alpha} \geq 0, \gamma^{\alpha} \geq 0, \varepsilon^{\alpha} \geq 0, b^{\alpha} \geq 0$ *then* $S_n \geq 0, I_n \geq 0, W_n \geq 0$, *for all* $n = 1, 2, 3, \ldots$ *with assumption of* $\Delta B_n = 0$.

Proof: For this, by using the Induction method we get

For $n = 0$,

$$S_1 = \frac{\nu_1 S_0 + \rho_1 S_0 + (\mathcal{K}(h))^{\alpha} (\Lambda^{\alpha})}{1 + (\mathcal{K}(h))^{\alpha} \left(\beta^{\alpha} I_0 e^{-(\mu^{\alpha}+\gamma^{\alpha})\tau} + \mu^{\alpha}\right)} \geq 0,$$

$$I_1 = \frac{\nu_1 I_0 + \rho_1 I_0 + (\mathcal{K}(h))^{\alpha} \left(\beta^{\alpha} S_1 I_0 e^{-(\mu^{\alpha}+\gamma^{\alpha})\tau}\right)}{1 + (\mathcal{K}(h))^{\alpha} (\gamma^{\alpha} + \varepsilon^{\alpha})} \geq 0,$$

$$W_1 = \frac{\nu_1 W_0 + \rho_1 W_0 + (\mathcal{K}(h))^{\alpha} (\varepsilon^{\alpha} I_1)}{1 + (\mathcal{K}(h))^{\alpha} (b^{\alpha})} \geq 0.$$

For $n = 1$,

$$S_2 = \frac{\nu_1 S_1 + \nu_2 S_0 + \rho_2 S_0 + (\mathcal{K}(h))^{\alpha} (\Lambda^{\alpha})}{1 + (\mathcal{K}(h))^{\alpha} \left(\beta^{\alpha} I_1 e^{-(\mu^{\alpha}+\gamma^{\alpha})\tau} + \mu^{\alpha}\right)} \geq 0,$$

$$I_2 = \frac{\nu_1 I_1 + \nu_2 I_0 + \rho_2 I_0 + (\mathcal{K}(h))^{\alpha} \left(\beta^{\alpha} S_2 I_1 e^{-(\mu^{\alpha}+\gamma^{\alpha})\tau}\right)}{1 + (\mathcal{K}(h))^{\alpha} (\gamma^{\alpha} + \varepsilon^{\alpha})} \geq 0,$$

$$W_2 = \frac{\nu_1 W_1 + \nu_2 W_0 + \rho_2 W_0 + (\mathcal{K}(h))^{\alpha} (\varepsilon^{\alpha} I_2)}{1 + (\mathcal{K}(h))^{\alpha} (b^{\alpha})} \geq 0.$$

For $n = 2$,

$$S_3 = \frac{\nu_1 S_2 + \nu_2 S_1 + \nu_3 S_0 + \rho_3 S_0 + (\mathcal{K}(h))^{\alpha} (\Lambda^{\alpha})}{1 + (\mathcal{K}(h))^{\alpha} \left(\beta^{\alpha} I_2 e^{-(\mu^{\alpha}+\gamma^{\alpha})\tau} + \mu^{\alpha}\right)} \geq 0,$$

$$I_3 = \frac{\nu_1 I_2 + \nu_2 I_1 + \nu_3 I_0 + \rho_3 I_0 + (\mathcal{K}(h))^{\alpha} \left(\beta^{\alpha} S_3 I_2 e^{-(\mu^{\alpha}+\gamma^{\alpha})\tau}\right)}{1 + (\mathcal{K}(h))^{\alpha} (\gamma^{\alpha} + \varepsilon^{\alpha})} \geq 0,$$

$$W_3 = \frac{\nu_1 W_2 + \nu_2 W_1 + \nu_3 W_0 + \rho_3 W_0 + (\mathcal{K}(h))^{\alpha} (\varepsilon^{\alpha} I_2)}{1 + (\mathcal{K}(h))^{\alpha} (b^{\alpha})} \geq 0.$$

Suppose that for $n = 1, 2, 3, \ldots, n-1$, $S_n \geq 0$, $I_n \geq 0$, and $W_n \geq 0$,

thus for $n = n$,

$$S_{n+1} = \frac{\sum_{i=1}^{n+1} v_i S_{n+1-i} - \rho_{n+1} S_0 + (\mathcal{K}(h))^{\alpha} (\Lambda^{\alpha})}{1 + (\mathcal{K}(h))^{\alpha} \left(\beta^{\alpha} I_n e^{-(\mu^{\alpha}+\gamma^{\alpha})\tau} + \mu^{\alpha}\right)},$$

$$I_{n+1} = \frac{\sum_{i=1}^{n+1} v_i I_{n+1-i} + \rho_{n+1} I_0 + (\mathcal{K}(h))^{\alpha} \left(\beta^{\alpha} S_{n+1} I_n e^{-(\mu^{\alpha}+\gamma^{\alpha})\tau}\right)}{1 + (\mathcal{K}(h))^{\alpha} (\gamma^{\alpha} + \varepsilon^{\alpha})},$$

$$W_{n+1} = \frac{\sum_{i=1}^{n+1} v_i W_{n+1-i} + \rho_{n+1} W_0 + (\mathcal{K}(h))^{\alpha} (\varepsilon^{\alpha} I_{n+1})}{1 + (\mathcal{K}(h))^{\alpha} (b^{\alpha})}.$$

As required. □

Theorem 11: *Suppose that* $S_0 + I_0 + W_0 = 1, \Lambda^{\alpha} \geq 0, \beta^{\alpha} \geq 0, \mu^{\alpha} \geq 0, \gamma^{\alpha} \geq 0, \varepsilon^{\alpha} \geq 0, b^{\alpha} \geq 0$ *and* $(\mathcal{K}(h))^{\alpha} \geq 0$ *then* S_n, I_n, W_n *are all bounded for all* $n = 1, 2, 3, \ldots, n$ *with assumption of* $\Delta B_n = 0$.

Proof: For this,

$$\begin{aligned}
&S_{n+1} + (\mathcal{K}(h))^{\alpha} \left(\beta^{\alpha} I_n e^{-(\mu^{\alpha}+\gamma^{\alpha})\tau} + \mu^{\alpha}\right) S_{n+1} + I_{n+1} + (\mathcal{K}(h))^{\alpha} (\gamma^{\alpha} + \varepsilon^{\alpha}) I_{n+1} + W_{n+1} + (\mathcal{K}(h))^{\alpha} (b^{\alpha}) W_{n+1} \\
&\quad = \sum_{i=1}^{n+1} v_i S_{n+1-i} - \rho_{n+1} S_0 + (\mathcal{K}(h))^{\alpha} (\Lambda^{\alpha}) + \sum_{i=1}^{n+1} v_i I_{n+1-i} + \rho_{n+1} I_0 + (\mathcal{K}(h))^{\alpha} \left(\beta^{\alpha} S_{n+1} I_n e^{-(\mu^{\alpha}+\gamma^{\alpha})\tau}\right) \\
&\quad + \sum_{i=1}^{n+1} v_i W_{n+1-i} + \rho_{n+1} W_0 + (\mathcal{K}(h))^{\alpha} (\varepsilon^{\alpha} I_{n+1}), \\
&\left(1 + (\mathcal{K}(h))^{\alpha} \left(\beta^{\alpha} I_n e^{-(\mu^{\alpha}+\gamma^{\alpha})\tau} + \mu^{\alpha}\right)\right) S_{n+1} + \left(1 + (\mathcal{K}(h))^{\alpha} (\gamma^{\alpha} + \varepsilon^{\alpha})\right) I_{n+1} + \left(1 + (\mathcal{K}(h))^{\alpha} (b^{\alpha})\right) W_{n+1} \\
&= \sum_{i=1}^{n+1} v_i \left(S_{n+1-i} + I_{n+1-i} + W_{n+1-i}\right) + \rho_{n+1} (S_0 + I_0 + W_0) + (\mathcal{K}(h))^{\alpha} \left(\Lambda^{\alpha} + \beta^{\alpha} S_{n+1} I_n e^{-(\mu^{\alpha}+\gamma^{\alpha})\tau} + \varepsilon^{\alpha} I_{n+1}\right).
\end{aligned}$$

Next, we use the Induction method to evaluate the further iteration then.

For $n = 0$,

$$\begin{aligned}
&\left(1 + (\mathcal{K}(h))^{\alpha} \left(\beta^{\alpha} I_0 e^{-(\mu^{\alpha}+\gamma^{\alpha})\tau} + \mu^{\alpha}\right)\right) S_1 + \left(1 + (\mathcal{K}(h))^{\alpha} (\gamma^{\alpha} + \varepsilon^{\alpha})\right) I_1 + \left(1 + (\mathcal{K}(h))^{\alpha} (b^{\alpha})\right) W_1 \\
&\quad = v_1 (S_0 + I_0 + W_0) + \rho_1 + (\mathcal{K}(h))^{\alpha} \left(\Lambda^{\alpha} + \beta^{\alpha} S_1 I_0 e^{-(\mu^{\alpha}+\gamma^{\alpha})\tau} + \varepsilon^{\alpha} I_1\right) \\
&\quad = v_1 + \frac{1}{\Gamma(1-\alpha)} + (\mathcal{K}(h))^{\alpha} \left(\Lambda^{\alpha} + \beta^{\alpha} S_1 I_0 e^{-(\mu^{\alpha}+\gamma^{\alpha})\tau} + \varepsilon^{\alpha} I_1\right) = \Upsilon_1,
\end{aligned}$$

$$\left(1 + (\mathcal{K}(h))^{\alpha} \left(\beta^{\alpha} I_0 e^{-(\mu^{\alpha}+\gamma^{\alpha})\tau} + \mu^{\alpha}\right)\right) S_1 \leq v_1 + \frac{1}{\Gamma(1-\alpha)} + (\mathcal{K}(h))^{\alpha} \left(\Lambda^{\alpha} + \beta^{\alpha} S_1 I_0 e^{-(\mu^{\alpha}+\gamma^{\alpha})\tau} + \varepsilon^{\alpha} I_1\right),$$

$$\left(1 + (\mathcal{K}(h))^{\alpha} (\gamma^{\alpha} + \varepsilon^{\alpha})\right) I_1 \leq v_1 + \frac{1}{\Gamma(1-\alpha)} + (\mathcal{K}(h))^{\alpha} \left(\Lambda^{\alpha} + \beta^{\alpha} S_1 I_0 e^{-(\mu^{\alpha}+\gamma^{\alpha})\tau} + \varepsilon^{\alpha} I_1\right),$$

$$\left(1 + (\mathcal{K}(h))^{\alpha} (b^{\alpha})\right) W_1 \leq v_1 + \frac{1}{\Gamma(1-\alpha)} + (\mathcal{K}(h))^{\alpha} \left(\Lambda^{\alpha} + \beta^{\alpha} S_1 I_0 e^{-(\mu^{\alpha}+\gamma^{\alpha})\tau} + \varepsilon^{\alpha} I_1\right),$$

$$S_1(t) \leq \frac{\Upsilon_1}{\left(1 + (\mathcal{K}(h))^{\alpha} \left(\beta^{\alpha} I_0 e^{-(\mu^{\alpha}+\gamma^{\alpha})\tau} + \mu^{\alpha}\right)\right)},$$

$$I_1(t) \leq \frac{\Upsilon_1}{\left(1 + (\mathcal{K}(h))^{\alpha} (\gamma^{\alpha} + \varepsilon^{\alpha})\right)},$$

$$W_1(t) \le \frac{\Upsilon_1}{\left(1+(\mathcal{K}(h))^{\alpha}(b^{\alpha})\right)},$$

$$S_1(t) \le \Upsilon_1, I_1(t) \le \Upsilon_1, R_1(t) \le \Upsilon_1.$$

For $n = 1$,

$$\begin{aligned}
&\left(1+(\mathcal{K}(h))^{\alpha}\left(\beta^{\alpha}I_1e^{-(\mu^{\alpha}+\gamma^{\alpha})\tau}+\mu^{\alpha}\right)\right)S_2+\left(1+(\mathcal{K}(h))^{\alpha}(\gamma^{\alpha}+\varepsilon^{\alpha})\right)I_2+\left(1+(\mathcal{K}(h))^{\alpha}(b^{\alpha})\right)W_3\\
&=\nu_1(S_1+I_1+W_1)+\nu_2(S_0+I_0+W_0)+\rho_2+(\mathcal{K}(h))^{\alpha}\left(\Lambda^{\alpha}+\beta^{\alpha}S_2I_1e^{-(\mu^{\alpha}+\gamma^{\alpha})\tau}+\varepsilon^{\alpha}I_2\right)\le\alpha(1)\\
&+\alpha(\Upsilon_1+\Upsilon_1+\Upsilon_1)+\frac{1}{\Gamma(1-\alpha)}+(\mathcal{K}(h))^{\alpha}\left(\Lambda^{\alpha}+\beta^{\alpha}S_2I_1e^{-(\mu^{\alpha}+\gamma^{\alpha})\tau}+\varepsilon^{\alpha}I_2\right)\le\alpha+3\alpha\Upsilon_1+\frac{1}{\Gamma(1-\alpha)}\\
&+(\mathcal{K}(h))^{\alpha}\left(\Lambda^{\alpha}+\beta^{\alpha}S_2I_1e^{-(\mu^{\alpha}+\gamma^{\alpha})\tau}+\varepsilon^{\alpha}I_2\right)\Upsilon_2,
\end{aligned}$$

$$\left(1+(\mathcal{K}(h))^{\alpha}\left(\beta^{\alpha}I_1e^{-(\mu^{\alpha}+\gamma^{\alpha})\tau}+\mu^{\alpha}\right)\right)S_2\le\alpha+3\alpha\Upsilon_1+\frac{1}{\Gamma(1-\alpha)}+(\mathcal{K}(h))^{\alpha}\left(\Lambda^{\alpha}+\beta^{\alpha}S_2I_1e^{-(\mu^{\alpha}+\gamma^{\alpha})\tau}+\varepsilon^{\alpha}I_2\right),$$

$$\left(1+(\mathcal{K}(h))^{\alpha}(\gamma^{\alpha}+\varepsilon^{\alpha})\right)I_2\le\alpha+3\alpha\Upsilon_1+\frac{1}{\Gamma(1-\alpha)}+(\mathcal{K}(h))^{\alpha}\left(\Lambda^{\alpha}+\beta^{\alpha}S_2I_1e^{-(\mu^{\alpha}+\gamma^{\alpha})\tau}+\varepsilon^{\alpha}I_2\right),$$

$$\left(1+(\mathcal{K}(h))^{\alpha}(b^{\alpha})\right)W_2\le\alpha+3\alpha\Upsilon_1+\frac{1}{\Gamma(1-\alpha)}+(\mathcal{K}(h))^{\alpha}\left(\Lambda^{\alpha}+\beta^{\alpha}S_2I_1e^{-(\mu^{\alpha}+\gamma^{\alpha})\tau}+\varepsilon^{\alpha}I_2\right),$$

$$S_2(t) \le \frac{\Upsilon_2}{\left(1+(\mathcal{K}(h))^{\alpha}\left(\beta^{\alpha}I_1e^{-(\mu^{\alpha}+\gamma^{\alpha})\tau}+\mu^{\alpha}\right)\right)},$$

$$I_2(t) \le \frac{\Upsilon_2}{\left(1+(\mathcal{K}(h))^{\alpha}(\gamma^{\alpha}+\varepsilon^{\alpha})\right)},$$

$$W_2(t) \le \frac{\Upsilon_2}{\left(1+(\mathcal{K}(h))^{\alpha}\left(\beta_2^{\alpha}I_1e^{-\mu_2^{\alpha}\tau}+\mu_2^{\alpha}\right)\right)},$$

$$S_2(t) \le \Upsilon_2, I_2(t) \le \Upsilon_2, W_2(t) \le \Upsilon_2.$$

Now, consider that

$$S_n(t) \le \Upsilon_n, I_n(t) \le \Upsilon_n, W_n(t) \le \Upsilon_n,$$

here,

$$\Upsilon_n = \alpha+3\alpha(\Upsilon_{n-1},+\Upsilon_{n-2},\ldots.\Upsilon_2+\Upsilon_1)+\frac{1}{\Gamma(1-\alpha)}+(\mathcal{K}(h))^{\alpha}\left(\Lambda^{\alpha}+\beta^{\alpha}S_{n+1}I_ne^{-(\mu^{\alpha}+\gamma^{\alpha})\tau}+\varepsilon^{\alpha}I_{n+1}\right).$$

For $n = n$,

$$\begin{aligned}
&\left(1+(\mathcal{K}(h))^{\alpha}\left(\beta^{\alpha}I_ne^{-(\mu^{\alpha}+\gamma^{\alpha})\tau}+\mu^{\alpha}\right)\right)S_{n+1}+\left(1+(\mathcal{K}(h))^{\alpha}(\gamma^{\alpha}+\varepsilon^{\alpha})\right)I_{n+1}+\left(1+(\mathcal{K}(h))^{\alpha}(b^{\alpha})\right)W_{n+1}\\
&=\textstyle\sum_{i=1}^{n+1}\nu_i(S_{n+1-i}+I_{n+1-i}+W_{n+1-i})+\rho_{n+1}(S_0+I_0+W_0)+(\mathcal{K}(h))^{\alpha}\left(\Lambda^{\alpha}+\beta^{\alpha}S_{n+1}I_ne^{-(\mu^{\alpha}+\gamma^{\alpha})\tau}+\varepsilon^{\alpha}I_{n+1}\right)\\
&=\nu_1(S_n+I_n+W_n)+\nu_2(S_{n-1}+I_{n-1}+W_{n-1})+\nu_3(S_{n-2}+I_{n-2}+W_{n-2})+\ldots+\nu_n(S_1+I_1+W_1)
\end{aligned}$$

$$+\nu_{n+1}\left(S_0+I_0+W_0\right)+\rho_{n+1}+\left(\mathcal{K}\left(h\right)\right)^{\alpha}\left(\Lambda^{\alpha}+\beta^{\alpha}S_{n+1}I_n e^{-\left(\mu^{\alpha}+\gamma^{\alpha}\right)\tau}+\varepsilon^{\alpha}I_{n+1}\right)\leq\alpha\left(3\Upsilon_n\right)+\alpha\left(3\Upsilon_{n-1}\right)$$

$$+\alpha\left(3\Upsilon_{n-2}\right)+\ldots+\alpha\left(3\Upsilon_2\right)+\alpha\left(3\Upsilon_1\right)+\alpha(1)+\frac{1}{\Gamma\left(1-\alpha\right)}+\left(\mathcal{K}\left(h\right)\right)^{\alpha}\left(\Lambda^{\alpha}+\beta^{\alpha}S_{n+1}I_n e^{-\left(\mu^{\alpha}+\gamma^{\alpha}\right)\tau}+\varepsilon^{\alpha}I_{n+1}\right)$$

$$\leq\alpha+\frac{1}{\Gamma\left(1-\alpha\right)}+3\alpha\left(\Upsilon_{n-1},+\Upsilon_{n-2},\ldots,\Upsilon_2+\Upsilon_1\right)+\left(\mathcal{K}\left(h\right)\right)^{\alpha}\left(\Lambda^{\alpha}+\beta^{\alpha}S_{n+1}I_n e^{-\left(\mu^{\alpha}+\gamma^{\alpha}\right)\tau}+\varepsilon^{\alpha}I_{n+1}\right)=\Upsilon_{n+1},$$

$$\left(1+\left(\mathcal{K}\left(h\right)\right)^{\alpha}\left(\beta^{\alpha}I_n e^{-\left(\mu^{\alpha}+\gamma^{\alpha}\right)\tau}+\mu^{\alpha}\right)\right)S_{n+1}\leq\alpha+\frac{1}{\Gamma\left(1-\alpha\right)}+3\alpha\left(\Upsilon_{n-1},+\Upsilon_{n-2},\ldots,\Upsilon_2+\Upsilon_1\right)$$

$$+\left(\mathcal{K}\left(h\right)\right)^{\alpha}\left(\Lambda^{\alpha}+\beta^{\alpha}S_{n+1}I_n e^{-\left(\mu^{\alpha}+\gamma^{\alpha}\right)\tau}+\varepsilon^{\alpha}I_{n+1}\right),$$

$$\left(1+\left(\mathcal{K}\left(h\right)\right)^{\alpha}\left(\gamma^{\alpha}+\varepsilon^{\alpha}\right)\right)I_{n+1}\leq\alpha+\frac{1}{\Gamma\left(1-\alpha\right)}+3\alpha\left(\Upsilon_{n-1},+\Upsilon_{n-2},\ldots,\Upsilon_2+\Upsilon_1\right)$$

$$+\left(\mathcal{K}\left(h\right)\right)^{\alpha}\left(\Lambda^{\alpha}+\beta^{\alpha}S_{n+1}I_n e^{-\left(\mu^{\alpha}+\gamma^{\alpha}\right)\tau}+\varepsilon^{\alpha}I_{n+1}\right),$$

$$\left(1+\left(\mathcal{K}\left(h\right)\right)^{\alpha}\left(b^{\alpha}\right)\right)W_{n+1}\leq\alpha+\frac{1}{\Gamma\left(1-\alpha\right)}+3\alpha\left(\Upsilon_{n-1},+\Upsilon_{n-2},\ldots,\Upsilon_2+\Upsilon_1\right)$$

$$+\left(\mathcal{K}\left(h\right)\right)^{\alpha}\left(\Lambda^{\alpha}+\beta^{\alpha}S_{n+1}I_n e^{-\left(\mu^{\alpha}+\gamma^{\alpha}\right)\tau}+\varepsilon^{\alpha}I_{n+1}\right),$$

$$S_{n+1}\leq\frac{\Upsilon_{n+1}}{\left(1+\left(\mathcal{K}\left(h\right)\right)^{\alpha}\left(\beta^{\alpha}I_n e^{-\left(\mu^{\alpha}+\gamma^{\alpha}\right)\tau}+\mu^{\alpha}\right)\right)},$$

$$I_{n+1}\leq\frac{\Upsilon_{n+1}}{\left(1+\left(\mathcal{K}\left(h\right)\right)^{\alpha}\left(\gamma^{\alpha}+\varepsilon^{\alpha}\right)\right)},$$

$$P_{n+1}\leq\frac{\Upsilon_{n+1}}{\left(1+\left(\mathcal{K}\left(h\right)\right)^{\alpha}\left(b^{\alpha}\right)\right)},$$

$$S_{n+1}\leq\Upsilon_{n+1},I_{n+1}\leq\Upsilon_{n+1},W_{n+1}\leq\Upsilon_{n+1},$$

As required. □

6 Numerical Simulations

The simulation parameter is explained in this section. The primary features of the simulated graphs are examined using the set of parametric variables given in Table 3. Furthermore, these graphs are created at the time when the disease is broadly exposed in the population and finally achieves a stable, present form. Appropriate values of α are selected at the current equilibrium to examine the dynamics of the disease.

Table 3: Values and description of variables and parameters

Variables/ Parameters	Descriptions	Values/Units	Source [1–24]
S	Susceptible cells at any time t	≥ 0	Assumption
I	Infected cells at any time t	≥ 0	Assumption
W	Immune cells at any time t	≥ 0	Assumption
Λ	The rate at which the susceptible blood cells enter into the circulatory blood.	0.5 cells^{-1}day^{-1} (The number of cells per microliter per day)	Estimated
μ	Mortality rates of susceptible blood cells.	0.5 day^{-1}	Fitted
β	Infection rate	1.05 cells^{-1}day^{-1} (The number of cells per microliter per day)	Estimated
ε	Recovery rate	0.001 cells^{-1}day^{-1} (The number of cells per microliter per day)	Fitted
γ	Mortality rates of infected cells.	0.5 day^{-1}	Fitted
b	Mortality rates of immune cells	0.03 day^{-1}	Estimated
σ_i	Rate of randomness in states variables	$0 \leq i \leq 1$	Fitted

Discussion

This section gives a detailed explanation of the graphs comparing the stochastic fractional delayed leukemia disease model for different values of the fractional order (α) with time delay $(\tau = 0.1)$, as discussed in the compartments like susceptible blood cells $S(t)$, infected cells $I(t)$, and immune cells $W(t)$. Fig. 3 depicts susceptible blood cell dynamics over time as a function of various values of fractional order (α). As shown in the figure for decreasing values of (α) from 0.9 to 0.5, it is slower because memory effects become dominant. For more significant values of (α), near 0.9, it reveals that susceptible blood cells decline more rapidly since they are transformed into infected cells. As (α) is decreased, past state effects increase and the susceptible blood cells grow infected with a delayed time period, while decline decreases in a more sustained way. It implies that lower fractional orders of response in the system introduce more delayed responses, simulating the slow onset of leukemia if historical states, or past immune responses and treatments, play a significantly higher role. Fig. 4 illustrates the dynamics of the infected cells versus time using several values of the fractional order (α). The dynamics of the infected cell population depend on (α) and are quite different at different values for (α). If the fractional order is fairly higher, say $(\alpha = 0.9)$, then the infected cell population is growing at a much higher rate and peaking to more pronouncedly higher values before stabilizing or decreasing. As (α) goes down, the rise in infected cells is more gradual. The peak values decrease if (α) is lower, indicating a delayed spread of infection. Lower values of (α) correspond to greater memory effects and a more drawn-out development of infected cells. This would therefore mean that when the value of (α) is lower, the disease develops slower, which might represent a delayed onset of leukemia because of the body's previous immunity responses or drug treatments. Fig. 5 depicts the dynamics of the immune cells for different values of the fractional order (α). The response curve of the immune system expressed through immune cells $W(t)$ is very much dependent on (α). When the value of (α) becomes higher, then the immune response will be quicker and more powerful, with immune cells building up a lot faster in a smaller amount of time to defeat the invading pathogens. When the value of (α) decreases, then the response of the immune system will be slower and even more feeble, producing fewer immune cells over time. That means the lower the fractional order, the later the response of the immune system: that is the influence of the progression of the disease and the memory of the immunity. It models the impact of past infection states

or treatments on the timing and the strength of the response from the immune system against leukemia. In higher fractional orders ($\alpha = 0.9$), these models have faster dynamics; susceptible cells become infected more rapidly, infection spreads quickly, and immune response is stronger as well as faster. This could thus describe an aggressive progression of leukemia with a robust initial immune response. At lower fractional orders ($\alpha = 0.5$), these models seem to reflect slower dynamics in which the progression of infected cells and the response by the immune system are postponed, indicating that memory effects from former immune activity or treatments are more important. This could be seen in some way as chronic or slow-moving leukemia in which the immune system takes a lot longer to react and the infection progresses slowly over time. The delay in the model and fractional orders highlights the effect of past behaviors and immune responses on the process of leukemia progression. Lower fractional orders reflect a more memorable system that delays transitions among states, such as susceptible to infection, causing the disease course to be much longer. It can be deduced that earlier interventions or immune responses may be the key to managing leukemia effectively.

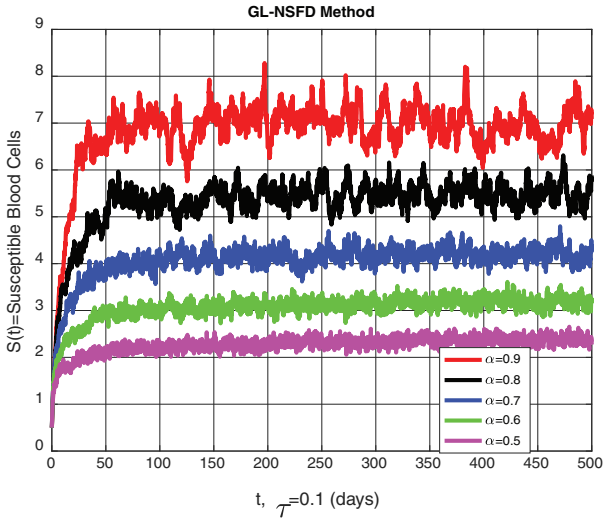

Figure 3: The susceptible blood cells are shown graphically for different values of fractional order (α)

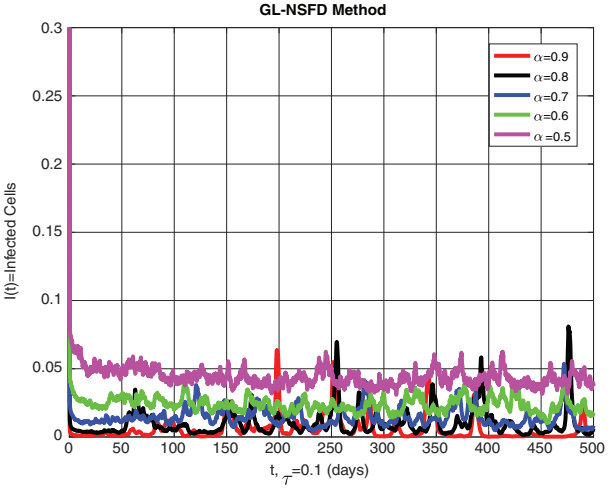

Figure 4: The infected cells are shown graphically for different values of fractional order (α)

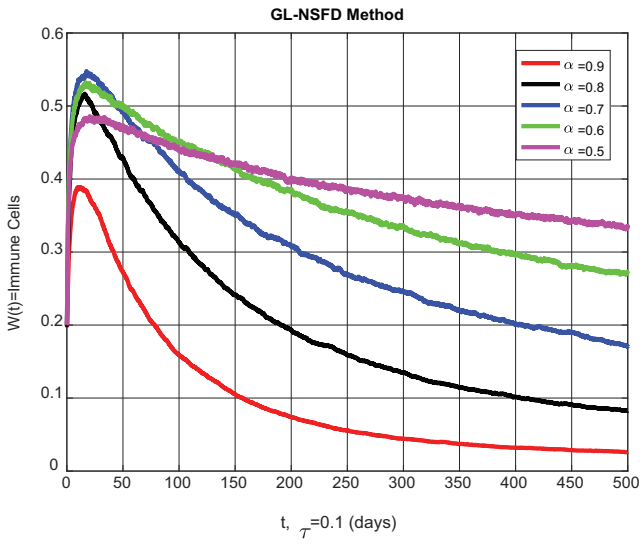

Figure 5: The immune cells' graphical behavior for different values of fractional order (α)

7 Conclusion

In this article, we have developed a stochastic fractional delayed model to examine the dynamics of leukemia. Thus, it provides significant insights into both the progression of the disease and its control mechanisms. The model (which is quite complex) is specifically designed to capture the intricate dynamics related to leukemia progression. It integrates delays and stochastic processes to address the variability that is inherent in the disease's advancement. A crucial aspect of this research involves identifying and analyzing both free and present equilibrium points, respectively. The computation of the reproduction number is essential for understanding the threshold behavior that determines whether the disease will persist or decline within a population. The stability of these equilibrium points (both locally and globally) is examined rigorously. Local stability, however, ensures the immediate response of the system around an equilibrium point. Global stability guarantees the system's long-term behavior. Interestingly, the results reveal critical conditions under which leukemia can be controlled or even eradicated. Although some parameters influence this stability, the underlying mechanisms remain complex. This complexity is vital because it shapes our understanding of potential therapeutic approaches. Sensitivity analysis further enhances these findings by identifying the key parameters that have the most significant influence on disease dynamics. This is crucial for developing targeted interventions (to effectively control the spread of leukemia). The GL-NSFD method is utilized for numerical simulations; it ensures the model's positivity and boundedness are both essential for maintaining biological relevance. The GL-NSFD method guarantees that solutions stay within realistic bounds, thus avoiding unphysical behavior in the simulation. However, graphical simulations are employed to substantiate the numerical findings, providing a visual representation of the model's behavior under various conditions. These simulations not only confirm the theoretical results but also demonstrate the practical applicability of the model for understanding leukemia dynamics. Although this research contributes valuable insights into leukemia modeling, it offers potential avenues for more effective treatment (and disease management strategies) because it lays the groundwork for future investigations.

Acknowledgement: This research was partially supported by the Fundacao para a Ciencia e Tecnologia, FCT, under the project https://doi.org/10.54499/UIDB/04674/2020 (accessed on 1 January 2025). Also, the authors were also partial supported by the Center for Research and Development in Mathematics and Applications (CIDMA) through the Portuguese Foundation for Science and Technology, references UIDB/04106/2020 and UIDP/04106/2020.

Funding Statement: This research was partially supported by the Fundação para a Ciência e Tecnologia, FCT, under the project https://doi.org/10.54499/UIDB/04674/2020 (accessed on 1 January 2025).

Author Contributions: Ali Raza: Conceptualization, Investigation, Data curation, Writing—original draft. Feliz Minhós: Project administration, Conceptualization, Investigation, Funding acquisition, Resources, Supervision. Umar Shafique and Muhammad Mohsin: Software, Writing—original draft & review & editing. All authors reviewed the results and approved the final version of the manuscript.

Availability of Data and Materials: All the data used and analyzed is available in the manuscript.

Ethics Approval: Not applicable.

Conflicts of Interest: The authors declare no conflicts of interest to report regarding the present study.

References

1. Khatun MS, Biswas MHA. Mathematical analysis and optimal control applied to the treatment of leukemia. J Appl Math Comput. 2020;64(1):331–53. doi:10.1007/s12190-020-01357-0.
2. Cadot S, Audebert C, Dion C, Ken S, Dupré L, Largeaud L, et al. New pharmacodynamic parameters linked with ibrutinib responses in chronic lymphocytic leukemia: prospective study in real-world patients and mathematical modeling. PLoS Med. 2024;21(7):e1004430. doi:10.1371/journal.pmed.1004430.
3. Kumar R, Shah SR, Stiehl T. Understanding the impact of feedback regulations on blood cell production and leukemia dynamics using model analysis and simulation of clinically relevant scenarios. Appl Math Model. 2024;129:340–89. doi:10.1016/j.apm.2024.01.048.
4. Parajdi LG, Bai X, Kegyes D, Tomuleasa C. A mathematical model of clonal hematopoiesis explaining phase transitions in myeloid leukemia. arXiv:2401.05316. 2024.
5. Brunetti M, Iasenza IA, Jenner AL, Raynal NJM, Eppert K, Craig M. Mathematical modeling of clonal reduction therapeutic strategies in acute myeloid leukemia. Leuk Res. 2024;140(4):107485. doi:10.1016/j.leukres.2024.107485.
6. Nicolini DL, Lepoutre T. Stability analysis of a model of INTERACTION between the immune system and cancer cells in chronic myelogenous leukemia. Bull Math Biol. 2018;80(5):1084–110. doi:10.1007/s11538-017-0272-7.
7. Serrano S, Barrio R, Martínez-Rubio Á, Belmonte-Beitia J, Pérez-García VM. Understanding the role of B-cells in CAR T-cell therapy in leukemia through a mathematical mode. arXiv:2403.00340. 2024.
8. Dariva K, Lepoutre T. Influence of the age structure on the stability in a tumor-immune model for chronic myeloid leukemia. Math Model Nat Phenom. 2024;19:1. doi:10.1051/mmnp/2023034.
9. Shah K, Ahmad S, Ullah A, Abdeljawad T. Study of chronic myeloid leukemia with T-cell under fractal-fractional order model. Open Phys. 2024;22(1):20240032. doi:10.1515/phys-2024-0032.
10. Lai X, Jiao X, Zhang H, Lei J. Computational modeling reveals key factors driving treatment-free remission in chronic myeloid leukemia patients. npj Syst Biol Appl. 2024;10(1):45. doi:10.1038/s41540-024-00370-4.
11. Zaagan AA, Mahnashi AM. Analysis of leukemia and forest fires data using new Poisson Quasi-Shanker distribution. Alex Eng J. 2024;104(3):701–9. doi:10.1016/j.aej.2024.08.012.
12. Bose P, Bandyopadhyay S. A comprehensive assessment and classification of acute lymphocytic leukemia. Math Comput Appl. 2024;29(3):45. doi:10.3390/mca29030045.
13. Li J, Pavlov S, Stakhov O. Expert systems for analysis of biomedical information in the diagnosis of acute leukemia. Інформаційні Технології Та Комп'ютерна Інженерія. 2024;59(1):157–64.
14. Miotto M, Scalise S, Leonetti M, Ruocco G, Peruzzi G, Gosti G. A size-dependent division strategy accounts for leukemia cell size heterogeneity. Commun Phys. 2024;7(1):248. doi:10.1038/s42005-024-01743-1.
15. Niño-López A, Chulián S, Martínez-Rubio Á, Blázquez-Goñi C, Rosa M. Mathematical modeling of leukemia chemotherapy in bone marrow. Math Model Nat Phenom. 2023;18:21. doi:10.1051/mmnp/2023022.
16. Abdullah R, Badralexi I, Halanay A. Stability analysis in a new model for desensitization of allergic reactions induced by chemotherapy of chronic lymphocytic leukemia. Mathematics. 2023;11(14):3225. doi:10.3390/math11143225.

17. Khan H, Alzabut J, Alfwzan WF, Gulzar H. Nonlinear dynamics of a piecewise modified ABC fractional-order leukemia model with symmetric numerical simulations. Symmetry. 2023;15(7):1338. doi:10.3390/sym15071338.
18. Pozzati G, Zhou J, Hazan H, Klement GL, Siegelmann HT, Tuszynski JA, et al. A systems biology analysis of chronic lymphocytic leukemia. Onco. 2024;4(3):163–91. doi:10.3390/onco4030013.
19. Jiwani N, Gupta K, Pau G, Alibakhshikenari M. Pattern recognition of acute lymphoblastic leukemia (ALL) using computational deep learning. IEEE Access. 2023;11:29541–53. doi:10.1109/access.2023.3260065.
20. Xiang H, Zhou M, Liu X. An optimal treatment strategy for a leukemia immune model governed by reaction-diffusion equations. J Dyn Control Syst. 2023;29(4):1219–39. doi:10.1007/s10883-022-09621-1.
21. Stiehl T. The multiplicity of time scales in blood cell formation and leukemia: contributions of computational disease modeling to mechanistic understanding and personalized medicine. In: Booß-Bavnbek B, Hesselbjerg Christensen J, Richardson K, Vallès Codina O, editors. Multiplicity of time scales in complex systems: challenges for sciences and communication I. Cham, Switzerland: Springer International Publishing; 2023. p. 327–99. doi: 10.1007/16618_2023_73.
22. Alsakaji HJ, Rihan FA, Udhayakumar K, El Ktaibi F. Stochastic tumor-immune interaction model with external treatments and time delays: an optimal control problem. Math Biosci Eng. 2023;20(11):19270–99. doi:10.3934/mbe.2023852.
23. Rihan FA, Udhayakumar K. Fractional order delay differential model of a tumor-immune system with vaccine efficacy: stability, bifurcation and control. Chaos Solitons Fractals. 2023;173(4):113670. doi:10.1016/j.chaos.2023.113670.
24. Moore H, Li NK. A mathematical model for chronic myelogenous leukemia (CML) and T cell interaction. J Theor Biol. 2004;227(4):513–23. doi:10.1016/j.jtbi.2003.11.024.